Dynamics of Contact Line Depinning from a Single Defect

J. A. Marsh* and A. M. Cazabat
Collège de France, Physique de la Matière Condensée, 11 Place Marcelin Berthelot, 75231 Paris Cedex 05, France
(Received 28 July 1993)

We examine the motion of the contact line as it is depinned from a single defect. The main features of the time evolution are in agreement with the "pinched cord" model of de Gennes. In particular, the contact line shape is well described by a logarithmic form with width increasing linearly and maximum distortion decreasing logarithmically in time. The velocity characteristic of the width increase, however, is larger than expected. Evidence is presented that this is a consequence of the role played by the dynamic contact angle in real situations, which is not accounted for in the present theory.

PACS numbers: 68.10.—m, 68.45.—v

Studies in dynamic wetting phenomena in near ideal situations have numerous potential applications in a variety of high technology manufacturing and coating processes, including, to name a few, microelectronics, photographic film, optical components, and both rigid and flexible magnetic storage media. These processes typically involve the spreading of liquids (lubricants, protective coatings, inks, etc.) on a controlled solid surface. Nonideality of a solid surface over which a contact line (where the liquid-air interface meets the solid surface) moves generally has a large effect on the efficiency and uniformity of such processes. More fundamentally, the existence of surface chemical heterogeneity and roughness are known [1] to be intimately linked to the existence of contact angle hysteresis, where the contact angle θ_0 depends on the previous history of the contact line motion. A quantitative experimental link between real surfaces (with typically random heterogeneities) and the resulting contact angle hysteresis has not yet been achieved. Analysis has focused on the single defect limit or on periodic defects, cases where some control over the heterogeneity is possible. Thus the dynamic response of the contact line to isolated heterogeneities is of interest both in itself and, ultimately, for a more fundamental understanding of contact angle hysteresis phenomena.

The *statics* of contact line pinning on single defects has recently received both theoretical and experimental study [2–6]. The principal results of these investigations are that the elasticity of the contact line has an unusual linear q dependence (q being the wave number of a small sinusoidal perturbation). Experiments have verified this property [3], as well as the predicted linear (i.e., Hookean) relation between the pinning force and maximum physical displacement [4]. For the case of complete wetting, theory [5] and experiment [6] indicate that the elasticity and force law are both modified to be cubic relations.

In this Letter, we present the first quantitative measurements, to our knowledge, of the *dynamics* of contact line depinning from a single defect. This represents an important step, as it addresses the contact line dynamics in a realistic situation not yet studied experimentally. Our main result is that the basic features of the relaxation process are well described by the theory of de Gennes [7]: After depinning, the contact line shape evolves following a logarithmic form with width increasing at a well defined characteristic velocity, and maximum height that decays logarithmically in time. The measured characteristic velocity, however, is an order of magnitude higher than predicted by theory, based on the best available data on viscous dissipation at a moving contact line. The implications of these results and a partial resolution to the anomalous characteristic velocity are discussed.

In what follows, we first briefly review the theory, then present a detailed analysis of our results for four representative events, at each of four fluid viscosities, with a vertical substrate (immersion angle $\alpha=0°$). We then present a summary of results for events with immersion angles $\alpha\neq 0°$.

Joanny and de Gennes [2] considered the case of an ideal (smooth, homogeneous) solid surface and a liquid with a small nonzero contact angle. By calculating the entire fluid-fluid interface shape when small periodic perturbations are made on a straight segment of contact line, they arrived at an elastic energy of the form

$$U_{\mathrm{cap}}=\frac{\gamma\theta_0^2}{2}\int_{-\infty}^{+\infty}|q||\tilde{\eta}_q|^2\frac{dq}{2\pi}, \tag{1}$$

where γ is the interfacial tension, θ_0 is the equilibrium contact angle, q is the wave number of the perturbation, and $\tilde{\eta}_q$ is the Fourier transform of the contact line distortion $\eta(x)$ (the equilibrium contact line is described by $\eta=0$). This energy is due entirely to capillary forces. Physically, it arises from the increase in surface area of the fluid-fluid interface.

As the deformed contact line relaxes, this elastic energy is dissipated in viscous flow. It is assumed that the contact angle is small and remains at the static value throughout the event. Then the lubrication approximation can be applied to the flow in this thin wedge [1], and the dissipation can be written as

$$\Sigma_w=\frac{3\mu U^2}{\theta_0}\ln\left[\frac{x_+}{x_-}\right]. \tag{2}$$

Here the speed of the contact line is U, μ is the fluid

0031-9007/93/71(15)/2433(4)$06.00

TABLE I. Summary of four representative events (from a set of 15) for four viscosities of PDMS, using a vertical plate. The relative reproducibility, from defect to defect, of the initial maximum distortion, c, H, l, and f are about 15%, 13%, 12%, 11%, and 3%, respectively. The contact angle measurements were performed using sessile drop goniometry and have an error of less than 0.5°.

Viscosity (cS)	Surface tension	Contact angle	Initial maximum distortion (cm)	Fitted c (cm/s)	Average H (cm)	Calculated l	Calculated f (dyn)
20	20.6	0°	0.025	0.072	0.0044	0	0
100	20.9	7.0	0.025	0.046	0.0040	0.27	0.0082
300	21.1	10.3	0.027	0.026	0.0048	0.53	0.019
500	21.1	10.7	0.024	0.017	0.0041	0.56	0.019

viscosity, and the logarithmic factor (henceforth denoted l) contains the ratio of the minimum to the maximum length scales over which the flow field is integrated. The minimum length scale is needed to avoid the well-known singularity at the moving contact line [8,9].

The rate of change in elastic energy is then equated to the viscous dissipation [7], yielding

$$\frac{\partial \tilde{\eta}_q}{\partial t} = -\left[\frac{\gamma \theta_0^3 |q|}{3\mu l}\right]\tilde{\eta}_q \equiv -c|q|\tilde{\eta}_q . \tag{3}$$

Here, c is a materials parameter with units of velocity. Individual modes thus decay exponentially with a $|q|$ dependent time constant $(c|q|)^{-1}$. If a localized (i.e., delta function) force of magnitude f is applied, and then released at time $t=0$, then the solution is

$$\eta(x,t>0) = \frac{-f}{2\pi\gamma\theta_0^2}\ln\left[\frac{x^2+(ct)^2}{L^2}\right]. \tag{4}$$

The term L is a long length scale cutoff determined by the outer geometry of the meniscus. This form is valid only for $x < L$. In the case of capillary rise on a homogeneous plate tilted at angle α with respect to the vertical, we expect $L = \kappa^{-1}(\cos\alpha)^{-1/2}$, where κ^{-1} is the capillary length $(\gamma/\rho g)^{1/2}$ (ρ is the fluid density and g is gravity).

The contact line shape given by Eq. (4) has width ct, increasing linearly with time, and maximum distortion $\eta(0,t) \sim -\ln(t)$.

The elastic energy given in Eq. (1) is strictly valid only when gravitational effects are negligible [10]. In our experiments, it would be immediately apparent if gravity were playing a significant role in the dynamics, because the differential equation [Eq. (3)] is changed. In particular, the width of the perturbation is no longer expected to increase linearly with time.

The experiments consisted of a quasistatic immersion of a treated silicon wafer into a bath of polydimethylsiloxane (PDMS, a silicon oil) at various immersion angles, ranging from $\alpha = 0°$ to 60°. The silicon wafer was treated [11] by hexadecyl-trichlorosilane leading to a chemically grafted C16 alkyl layer, a low energy surface. The wafer was cleaned using chloroform in an ultrasonic bath. Four different kinematic viscosities were used: 20, 100, 300, and 500 cS (1 cS$\equiv 10^{-2}$ cm^{2}s) (Rhodorsil 47-V series, Prolabo, France), with known surface tensions of 20.6, 20.9, 21.1, and 21.1 dynes/cm, respectively. We use the quoted values of viscosity and surface tension, which have an accuracy of about 10% and 2%, respectively. Table I gives the measured contact angles on the wafer. Clearly the assumption of a small *static* contact angle is satisfied.

Nonwetting defects were made with Staedtler projector pen ink, as described in previous studies [6,12]. The wafer was advanced into the silicon oil until the contact line was close to depinning from the top of a vertical line defect with a circular tip 0.3–0.5 mm in diameter. See Fig. 1. The wafer was then advanced in very small increments (≈ 20 μm) until the contact line engulfed the defect. Once it passed the defect, the contact line relaxed freely on the surface. This relaxation constitutes the depinning event and was captured and analyzed using video microscopy. For each event about twenty photos were analyzed, over a total time appropriate to the duration of the event. Each event analyzed uses a different defect, because they were dissolved upon cleaning the wafer.

The experimental contact line shapes were individually fitted to the function

$$\eta(H,W,L) = -H\ln\left[\frac{x^2+W^2}{L^2}\right], \tag{5}$$

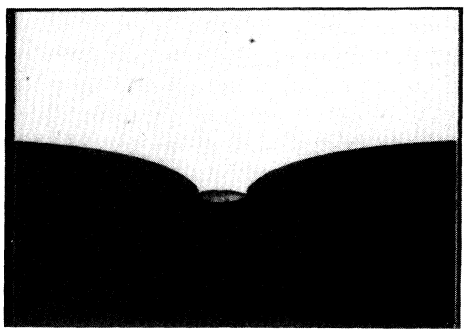

FIG. 1. A contact line configuration shortly before the depinning event occurs, showing the tip of the defect. The visible region is about 1.6 mm wide.

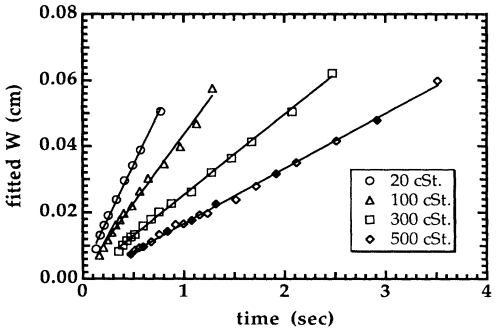

FIG. 2. The fitted width W plotted against time for four typical events, one at each viscosity. Error bars are slightly smaller than the symbol size. The origin in time for each event has been shifted to correspond to zero initial width. Linear best fits are shown as solid lines.

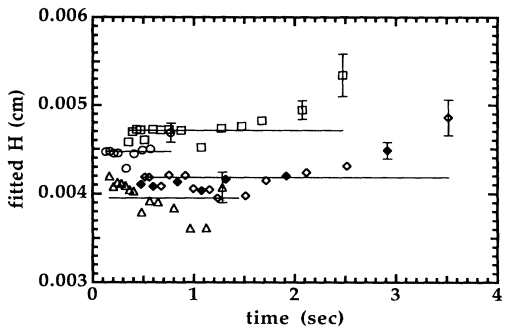

FIG. 3. The fitted parameter H plotted against time for the same events as in Fig. 2 (the same symbols are also used). Error bars are slightly smaller than the symbol size, except for those shown. Shown as the solid line is the average H value.

which is a generic form of Eq. (4). In the fits, the value of L was fixed at the expected value $\kappa^{-1}(\cos\alpha)^{-1/2}$.

Figures 2 and 3 display the fitted parameters W and H plotted against time for four typical events. For each event shown, the origin in time is shifted so $t=0$ corresponds to the origin in time in the theory. The finite initial width results from the finite-sized defect. W is to be identified with ct in Eq. (4), and H is to be identified with $f/2\pi\gamma\theta_0^2$. Thus we expect W to increase linearly in time, and for H to be constant. The expected behavior is observed: The characteristic velocity is very well defined, and the fitted H values are constant to about 10% accuracy. Shown as solid lines are fits which give the values for c and H reported in Table I. Using these values of c and H, it is possible to reconstruct the best "global" fit time series which evolves according to theory. An example is shown in Fig. 4.

Note that the $-\ln(t)$ behavior of the maximum distortion follows from these relations.

Three distinct regimes in time can be identified in our fits. In the first, typically for the first 0.5 sec after depinning, a transient occurs, during which χ^2 values are significantly greater than unity (based on an error of ± 0.5 pixels in the location of the contact line in the photos). After the transient, the χ^2 values stabilize at unity (which *only* happens if L has the value given above). Finally, the width W saturates to a constant value (on the order of the half-width of our data set) as the contact line shape becomes very flat, and the subsequent fits are dominated by noise. Only the data for times corresponding to W less than the saturated value are shown in the figures.

During the transient we observe significant disagreement with the logarithmic form 5, based on the χ^2 criteria. We attribute this to the finite width defect: The initial contact line shape after depinning depends on the shape of the defect, and is simply not equal to the theoretical shape. Even during the transient, however, the overall dimensions of the contact line distortion are well described by Eq. (5). In particular, the fitted H and W still provided a valid characterization of the contact line shape (see Fig. 4), and were thus used in the analysis.

As the width saturated, the fitted H values tended to deviate from a constant value. We believe this is an artifact of the finite width of the data set. As the spread in the fitted values is larger than the error bars can account for, there is noise in the data which is not accounted for by the simple pixel error mentioned above. This error clearly increases with time as the contact line flattens out, and is probably associated with the limitations of frame-by-frame transfer from video tape to the computer.

Our experimentally measured values of c allow us to evaluate, for those samples with $\theta_0 \neq 0$, the logarithmic dissipation factor l. Calculated values are shown in Table I, and are typically somewhat less than unity. Because of the restrictions on the sizes of the inner and outer cutoff distances, the generally accepted value of this quantity is in the range 10–15. For example, in an experimental study which directly addresses the hydrodynamics near a moving contact line [13], l was found to be about 12, giving a ratio $x_+/x_- \approx 10^{-5}$. This is for PDMS on bare Pyrex. For silicon wafers with coatings similar to ours,

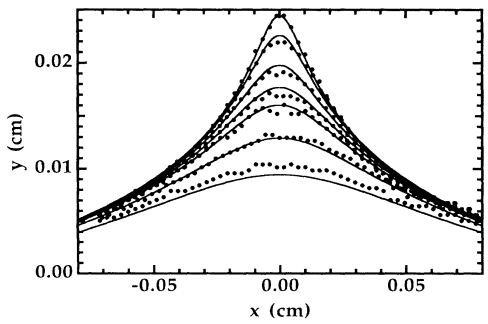

FIG. 4. A theoretical time series compared to the data, using the best fit *constants* for prefactor H and characteristic velocity c. Only one contact line shape in three is shown, identified by the filled data points in Figs. 2 and 3.

studies in which l has appeared as a parameter have yielded values ranging from 6 to 34 [3,14]. The very low values we find for l would imply an anomalously small dissipation in spreading [15]. We conclude that we have found a significant disagreement with the theory: Our experimental values of c are much larger than predicted.

The most plausible explanation for this disagreement is the fact that the contact angle *does not* remain at the static value throughout the event, as is assumed by theory. Because we do not have a direct measure of the contact angle during the event, we make an estimation based on the observed contact line velocity. It is well known [9] that the dynamic contact angle θ_{dyn} is equal to θ_0 only for capillary numbers less than about 1×10^{-5}. However, during our events we find capillary numbers as large as 5×10^{-3}. The usual Tanner law [1] predicts dynamic contact angles of up to 45° in this case. This provides a qualitative explanation for the high characteristic velocity we observe. However, because of the variation of Ca in both space and time during the event, it is not straightforward to generalize the theory to properly account for θ_{dyn}. In fact, it is remarkable that the theory works as well as it does, because it assumes not only a constant but also a very small contact angle.

Perhaps the strongest evidence that the dynamic contact angle is playing an important role is that our fits hold even for the 20 cS PDMS, which has a static contact angle of 0°. The theoretical description is not expected to apply at all in such cases of complete wetting. This is an example of the general fact that the distinction between wetting and nonwetting fluids tends to break down when moving contact lines are involved.

In light of the above discussion, there is clearly some question as to the validity of using θ_0 in evaluating the force parameter f $(=2\pi\gamma\theta_0^2H)$ from the experimental values of H. The results of this calculation are shown in Table I. The systematic rise in the force parameter with viscosity is due mainly to the quadratic dependence on θ_0, because all the fluids have essentially the same surface tension and all the events had the same maximal distortion at $x=0$ (see Table I). These values are consistent with the fact that the defects all had similar shape and size.

As the immersion angle increases, the transient became more long lived, until at $\alpha=60°$ it overlapped with the saturation for most events. The origin of this behavior is unknown. However, as the tilt angle was changed, two quantitative results were obtained (we merely quote the results here): (1) The characteristic velocity is still well defined, and is unchanged by the tilt; and (2) the appropriate cutoff length L changes in the expected way, scaling as $\kappa^{-1}(\cos\alpha)^{-1/2}$.

In conclusion, we have made a comparison with the "pinched cord" model of de Gennes describing contact line depinning from a localized pinning force. Most of the predictions of the theory are well verified: The time evolution of the distortion follows a logarithmic form, with cutoff length given by the capillary length (appropriately modified to reflect the imposed tilt), width increasing linearly in time, and maximal distortion following a logarithmic decay in time. The characteristic velocity of width increase, however, is an order of magnitude larger than predicted by theory. The influence of the dynamic contact angle is clear, and provides a qualitative explanation of the large characteristic velocity we obtain. We believe a suitable explanation for the viscosity and immersion angle dependence of our results also relies on a theory which properly accounts for the effects of the dynamic contact angle. These results provide important new information about the time and length scales involved in such depinning events.

The authors wish to thank S. Garoff, T. Ondarçuhu, E. Raphael, and M. O. Robbins for useful discussions.

*Present address: Arts and Sciences, SUNY Institute of Technology at Utica/Rome, Utica, New York 13504.

[1] P. G. de Gennes, Rev. Mod. Phys. **57**, 827 (1985).
[2] J. F. Joanny and P. G. de Gennes, J. Chem. Phys. **81**, 552 (1984).
[3] T. Ondarçuhu and M. Veyssié, Nature (London) **352**, 418 (1991).
[4] G. D. Nadkarni and S. Garoff, Europhys. Lett. **20**, 523 (1992).
[5] E. Raphael and J. F. Joanny, Europhys. Lett. **21**, 483 (1993).
[6] J. A. Marsh and A. M. Cazabat, Europhys. Lett. **23**, 45 (1993).
[7] P. G. de Gennes, C.R. Acad. Sci., Ser. II **302**, 731 (1986).
[8] C. Huh and L. E. Scriven, J. Colloid Interface Sci. **35**, 85 (1971).
[9] E. B. Dussan V., Annu. Rev. Fluid Mech. **11**, 371 (1979).
[10] Gravity modifies the q dependence of the elasticity for wave vectors smaller than κ. See [3], and Y. Pomeau and J. Vannimenus, J. Colloid Interface Sci. **104**, 477 (1985); F. Brochard and P. G. de Gennes, Langmuir **7**, 3216 (1991).
[11] Courtesy of J. B. Brzozka.
[12] A. M. Cazabat and F. Heslot, Colloids Surfaces **51**, 309 (1990).
[13] J. A. Marsh, S. Garoff, and E. B. Dussan V., Phys. Rev. Lett. **70**, 2778 (1993).
[14] C. Redon, F. Brochard-Wyart, and F. Rondelez, Phys. Rev. Lett. **66**, 715 (1991).
[15] It has been shown [16] that the dissipation at the front of a spreading monolayer can be anomalously small due to molecular effects. However, in the case of a macroscopic advancing wedge, a reduced molecular contribution cannot reduce the total dissipation below the viscous contribution.
[16] M. Cieplak, E. Smith, and M. O. Robbins, Nature (London) (to be published), and references therein.

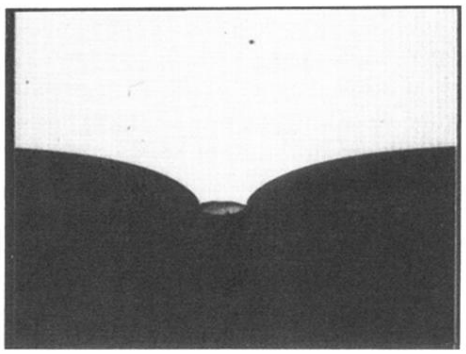

FIG. 1. A contact line configuration shortly before the depinning event occurs, showing the tip of the defect. The visible region is about 1.6 mm wide.